Potential effect and mechanism of ultrashort wave therapy in mice with chronic rhinosinusitis

HUIFANG XU, JING WENG, QUAN BAO, YUQIANG JIANG, CONG XIAO and LIUJUN CHEN

Department of Pediatrics, Lanxi People's Hospital, Lanxi, Zhejiang 321100, P.R. China

Received March 2, 2025; Accepted August 20, 2025

DOI: 10.3892/br.2026.2109

Abstract. Rhinosinusitis is an inflammatory condition that impacts both the nasal passages and the paranasal sinuses. Currently, there is no systematic or standardized treatment protocol for paediatric chronic rhinosinusitis (CRS). The aim of the present study was to conduct a preliminary investigation of the role and mechanism of ultrashort wave therapy in mice with CRS. Haematoxylin and eosin staining was performed to observe histopathological changes. Terminal deoxynucleotidyl transferase nick-end labelling assay was used to assess apoptosis in the sinus mucosa. Both immunofluorescence and enzyme-linked immunosorbent assay were performed to evaluate the expression levels of IFN-γ, IL-1α, TNF-α, and IL-10. Proteins associated with the p38/JNK/ERK signalling pathway were assessed using western blotting. The results revealed that ultrashort wave therapy significantly improved the histopathology of the sinus mucosa, particularly in maintaining the integrity of the ciliary structures. In addition, ultrashort wave therapy stimulated a notable decrease in apoptosis and inflammation in sinus mucosa samples. The phosphorylation levels of p38, JNK, and ERK were markedly inhibited in the sinus mucosa of mice with CRS subjected to ultrashort wave intervention. The findings of the present study elucidate a preliminary mechanism underlying the effects of ultrashort wave therapy on CRS progression. This suggests that ultrashort waves may be conducive to maintaining the integrity of the ciliary structures, inhibiting apoptosis, and reducing inflammation in the sinus mucosa. These effects are likely mediated through the inhibition of the p38/JNK/ERK signalling pathway.

Introduction

Rhinosinusitis is an inflammatory condition that affects both the nasal passages and paranasal sinuses. Chronic rhinosinusitis (CRS) occurs frequently in both adult and paediatric populations (1). Although the clinical manifestations of CRS may exhibit similarities, there are significant differences between adult and paediatric CRS across various dimensions. The diagnostic criteria for adults include hyposmia, facial pain/pressure, and nasal discharge or blockage (2). In paediatric populations, coughing has emerged as a substitute for reduced olfactory function (3). This finding was corroborated by a study that evaluated the clinical features of paediatric CRS, which revealed that the most frequently reported symptoms in children with CRS were a runny nose (96%) and cough (88%) (4). Currently, there is no systematic or standardised treatment protocol for paediatric CRS. The most commonly used interventions include nasal saline irrigation and intranasal corticosteroid administration, which have demonstrated therapeutic benefits in clinical practice (5). However, long-term outcomes remain suboptimal. Therefore, it is crucial to develop consensus-based guidelines for effective management of paediatric CRS to minimise its impact during childhood.

During the 20th century, physical therapists frequently employed thermotherapy utilising electromagnetic fields such as those from ultrashort-wave diathermy to manage painful musculoskeletal conditions (6). This treatment approach was a widely adopted modality within the field of physical therapy. Over the past 12 years, ultrashort waves have been used to treat various inflammatory diseases. For example, Yang *et al* (7) found that ultrashort waves interact with heat shock protein 70 to ameliorate pulmonary inflammation in mice with acute lung injury. In 2020, during the peak of the COVID-19 pandemic, some studies reported that ultrashort waves, as an alternative therapy, could inhibit inflammation and enhance immune responses (8). Nasal ultrashort wave therapy involves the placement of two electrodes on either side of the nose of the child, followed by adjustment of a high-frequency electric field. This process causes molecules within the nasal cavity and mucosa of the child to oscillate repeatedly in the horizontal direction. The friction generated between these molecules produces heat, which enhances the permeability of the nasal blood vessels, improves microcirculation, and promotes movement within the nasal mucosa. This accelerates the clearance of nasal secretions. Furthermore, ultrashort waves possess antibacterial properties that can eliminate certain bacteria, while inhibiting their growth and reproduction. This action helps suppress the development of inflammation and contributes to achieving a therapeutic effect. Currently numerous

Correspondence to: Dr Huifang Xu, Department of Pediatrics, Lanxi People's Hospital, 896 Huancheng West Road, Lanxi, Zhejiang 321100, P.R. China
E-mail: xhf_1122@163.com

Key words: chronic rhinosinusitis, ultrashort wave, sinus mucosa, apoptosis, inflammation

studies have confirmed the efficacy of ultrashort-wave therapy on CRS (9,10). However, the mechanism of action of ultrashort waves in paediatric patients with CRS remains elusive.

In the present study, a mouse model of CRS was developed, and an ultrashort-wave intervention was administered. The aim of the pesent study was to preliminarily explore the role and mechanism of ultrashort-wave therapy on CRS.

Materials and methods

Establishment of a CRS model in mice and ultrashort wave therapy. All experimental procedures involving mice adhered to the guidelines outlined in the National Institutes of Health Guide for the Care and Use of Laboratory Animals (11) and were approved (approval no. 20220601001) by the Ethics Committee of Lanxi People's Hospital (Lanxi, China). For this experiment, SLAC Laboratory Animal Co., Ltd. supplied 24 adult male C57BL/6J mice, aged 8-10 weeks and weighing between 24 and 27 g. All the mice were housed in specific pathogen-free environments under standard laboratory conditions. These conditions included a 12-h light/dark cycle, relative humidity maintained between 40 and 55%, and temperatures ranging from 22 to 25˚C. The animals had *ad libitum* access to food and water. All mice exhibited a good mental state and showed no signs of nasal congestion, rhinorrhoea, or sneezing. A week later, the mice were randomly and evenly divided into four groups: Control, sham, CRS, and CRS + ultrashort wave, with six mice in each group. The CRS model was established as previously described (12) with certain modifications. Briefly, following the administration of an intraperitoneal injection of pentobarbital sodium (50 mg/kg) for anaesthesia, a surgical incision was made from the right side of the snout, extending to the nasal bridge, to expose the right bony external nares. A Merocel nasal pack (5 mm; Medtronic, Inc.) that had been saturated with a solution of *Streptococcus pneumoniae* (20 μl; cat. no. BNCC360198; BeNa Culture Collection) was placed into the right nasal cavity, after which the incision was closed with sutures. For the mice in the sham group, a Merocel nasal pack was impregnated with sterile saline and placed in the right nasal cavity. Mice in the control group were not subjected to any treatment. Successful modelling was assessed based on symptoms observed in the mice, including nasal congestion, rhinorrhoea, and nose scratching. Mice in the CRS + ultrashort wave group underwent ultrashort wave intervention using an Ultrashort Wave Therapeutic Instrument (Model DL-C; Shantou Medical Equipment Factory Co., Ltd.) for 15 min per day over a duration of 12 weeks, starting 24 h post-modelling. The instrument needed to preheat for 5 min prior to ultrashort wave therapy. Subsequently, two circular electrodes, each with a diameter of 4 cm, were positioned parallel to one another on either side of the mouse's nose, ensuring a separation distance of ~2 cm. The ultrashort wave frequency was set at 40.68 MHz. The other groups did not receive any interventions. During this experiment, concerted efforts were made to minimise animal suffering. Subsequently, all the mice were euthanised by intraperitoneal injection of pentobarbital sodium (200 mg/kg). The nasal cavity was then rinsed to collect the nasal lavage fluid (NLF), and sinus mucosal samples were obtained for further analysis.

Haematoxylin and eosin (H&E) staining. Sinus mucosal specimens were processed by fixation (4% paraformaldehyde at 25˚C for 12 h), dehydration, and paraffin embedding. Following sectioning into 4-μm thick slices, the samples underwent dewaxing and rehydration before being stained with an H&E staining kit (cat. no. ab245880; Abcam) at 25˚C for 60 min. Images were acquired using a light microscope (Olympus Corporation).

Immunofluorescence. Sinus mucosal sections (4 μm) underwent deparaffinization in xylene for 10 min at room temperature and rehydration with descending concentrations of ethanol (100, 95, 70% for 3-5 min each), followed by antigen retrieval in heated citrate buffer (10 mM; pH 6.0) at 80˚C for 25 min. Subsequently, the samples were washed three times with PBS before being permeabilized using 0.5% Triton X-100 in PBS. The sections were then blocked with 5% BSA (cat. no. ST023; Beyotime Institute of Biotechnology) at room temperature for 1 h. Next, the sections were incubated with primary antibodies against IFN-γ (cat. no. 15365-1-AP), IL-1α (cat. no. 83644-1-RR), TNF-α (cat. no. 17590-1-AP), and IL-10 (cat. no. 60269-1-Ig) (all diluted 1:50; Proteintech Group, Inc.). Subsequently, they were labelled with an Alexa Fluor 568-conjugated secondary antibody (cat. no. A-11011; diluted 1:200; Invitrogen; Thermo Fisher Scientific, Inc.). Following DAPI staining (at room temperature for 15 min), fluorescence images of the sections were acquired under a fluorescence microscope (Model BX53; Olympus Corporation) and analysed using ImageJ software (version 1.8.0; National Institutes of Health).

Terminal deoxynucleotidyl transferase dUTP nick end labelling (TUNEL) assay. Sinus mucosa apoptosis was evaluated using the TUNEL Cell Apoptosis kit (Beijing Solarbio Science & Technology Co., Ltd.) according to the manufacturer's instructions. Briefly, the sinus mucosa tissues were fixed using 4% paraformaldehyde (48 h at 4˚C), embedded in paraffin and cut into 4-μm sections. The deparaffinized tissue sections were incubated with 3% hydrogen peroxide in methanol for 10 min at 25˚C in the dark, washed three times with PBS and incubated with 0.1% Triton X-100 in freshly prepared 0.01% sodium citrate for 8 min at 25˚C. Tissue sections were then incubated with proteinase K working solution for 25 min at 37˚C and washed three times with PBS (pH 7.4) for 5 min each. A total of 50 μl TUNEL reagent was added to each sample and incubated at 37˚C for 60 min. The sections were washed three times with PBS (pH 7.4) and then cell nuclei were counterstained with 2 μg/ml DAPI solution at room temperature for 10 min in the dark and mounted with 50 μl anti-fade mounting medium. Fluorescence images were obtained in five randomly-selected fields under an OLYMPUS fluorescence microscope (Model BX53) and analysed using ImageJ software (version 1.8.0; National Institutes of Health). The percentages of TUNEL-positive cells were assessed and presented as the apoptosis rate (%).

Enzyme-linked immunosorbent assay (ELISA). According to manufacturer's instructions, the concentrations of IFN-γ (cat. no. KTE7003; Abbkine Scientific Co., Ltd.), IL-1α (cat. no. ED-20161), TNF-α (cat. no. ED-20852), and IL-10

(cat. no. ED-20162; all from Xiamen LunChangShuo Biotechnology Co., Ltd.) in NLF were determined through the corresponding commercial kits.

Western blotting. Following incubation with RIPA lysis buffer (Biosharp Life Sciences), total protein was extracted from the sinus mucosal samples and quantified using a bicinchoninic acid kit. Next, 25 μg of protein per well was loaded and separated via 10% polyacrylamide gel electrophoresis before being transferred onto PVDF membranes. The membranes were blocked for 1 h at 25˚C with a 5% skim milk solution (Biosharp Life Sciences). This was succeeded by an overnight incubation at 4˚C with the respective primary antibodies. The membranes were then incubated for an additional hour with the corresponding secondary antibodies (cat. no. A21020; diluted 1:10,000; Abbkine Scientific Co., Ltd.). For detection purposes, the membranes were treated with SuperKine™ West Pico PLUS Chemiluminescent Substrate (Abbkine Scientific Co., Ltd.) and subsequently visualised utilising the ChemiDoc imaging system (Bio-Rad Laboratories, Inc.). The resulting images were analysed using the ImageJ software (version 1.8.0). A detailed account of the specific primary antibodies used in western blot analysis is presented in Table I.

Statistical analysis. *In vivo* experiments were performed using six mice per group. Each experiment was performed in triplicate. Data analysis was performed using SPSS software version 22.0 (IBM Corp.). To evaluate the differences among the data, one-way analysis of variance (ANOVA) followed by Tukey's post hoc multiple comparison test was applied. The results are presented as the mean ± standard deviation. P<0.05 was considered to indicate a statistically significant difference.

Results

Ultrashort wave therapy improves histopathology and inhibits apoptosis in sinus mucosal samples. H&E staining was employed to observe the histopathology of sinus mucosal samples. As illustrated in Fig. 1A, the epithelial cells in the sinus mucosa of control mice were orderly arranged, with no evidence of inflammatory cell infiltration observed in either the mucosa or submucosa. The sinus mucosal epithelial cells and ciliary structures in the sham group appeared intact and well-arranged, with sporadic goblet cells present in the submucosal layer. By contrast, the nasal sinus mucosa of mice with CRS exhibited signs of chronic inflammation, characterized by a disordered arrangement of mucosal epithelial cells, cilia shedding, partial cell necrosis, and significant lymphocytic infiltration. Following ultrashort wave therapy, there was an observable improvement in both the integrity of mucosal and ciliary structures as well as a reduction in lymphocyte numbers within the submucosal layer. The subsequent TUNEL assay was conducted to evaluate the apoptosis of sinus mucosal samples. The results indicated that there were no significant differences in the apoptosis rate between the control and sham groups. In comparison to the sham group, a notable increase in the apoptosis rate was observed in the CRS group (Fig. 1B and C; P<0.0001); however, this increase was partially mitigated following intervention with ultrashort wave therapy (P<0.01).

Table I. Primary antibodies used in western blotting.

Primary antibody	Cat. no.	Dilution ratio	Source
p38	66234-1-Ig	1:4,000	Proteintech Group, Inc.
p-p38	28796-1-AP	1:2,000	Proteintech Group, Inc.
JNK	66210-1-Ig	1:1,000	Proteintech Group, Inc.
p-JNK	60666-1-Ig	1:1,000	Proteintech Group, Inc.
ERK	16443-1-AP	1:2,000	Proteintech Group, Inc.
p-ERK	28733-1-AP	1:2,000	Proteintech Group, Inc.
GAPDH	60004-1-Ig	1:50,000	Proteintech Group, Inc.

Ultrashort wave therapy inhibits inflammatory responses in the sinus mucosal samples of mice with CRS. The expression levels of the anti-inflammatory cytokine IL-10, alongside pro-inflammatory cytokines such as IFN-γ, IL-1α, and TNF-α, were subsequently assessed in the sinus mucosal samples obtained from mice (Fig. 2A). No significant differences were found in the expression levels of IFN-γ, IL-1α, TNF-α, and IL-10 between the control and sham groups. The CRS group exhibited a marked increase in the expression levels of IFN-γ, IL-1α and TNF-α (Fig. 2B-D; P<0.01), along with a significant decrease in the expression of IL-10 (Fig. 2E; P<0.01), when compared with the sham group. Following ultrashort wave therapy, these expression changes were significantly reversed (Fig. 2B-E; P<0.05). Comparable patterns were noted in the concentrations of IFN-γ, IL-1α, TNF-α, and IL-10 in the NLF samples (Fig. 2F-I; P<0.05).

Ultrashort wave therapy inhibits the p38/JNK/ERK pathway in mice with CRS. The activation of MAPK pathway, which encompasses p38, JNK and ERK, plays a crucial role in regulating apoptosis as well as the release of pro-inflammatory cytokines (13). Subsequently, the effects of ultrashort wave therapy on the p38/JNK/ERK signalling pathway were investigated in mice with CRS. As illustrated in Fig. 3A, the protein levels of p38, JNK and ERK across the various groups exhibited no significant changes. However, the expression levels of phosphorylated proteins including p-p38, p-JNK and p-ERK were significantly increased in the CRS group compared with the sham group (P<0.01). By contrast, the expression levels of p-p38, p-JNK and p-ERK were significantly reduced when treated with ultrashort wave treatment (P<0.05). In addition, a significant upregulation in the ratios of p-p38/p38, p-JNK/JNK and p-ERK/ERK was observed in the CRS group (Fig. 3B; P<0.01). By contrast, these ratios were significantly reduced in the CRS + ultrashort wave group (P<0.05).

Discussion

CRS significantly impacts the quality of life and hinders the social functioning of affected individuals (14). Of particular concern is paediatric CRS, which imposes a considerable financial burden and strains healthcare resources due to its widespread prevalence. A previous study revealed that in the United States, there are approximately 3.7 to 7.5 million

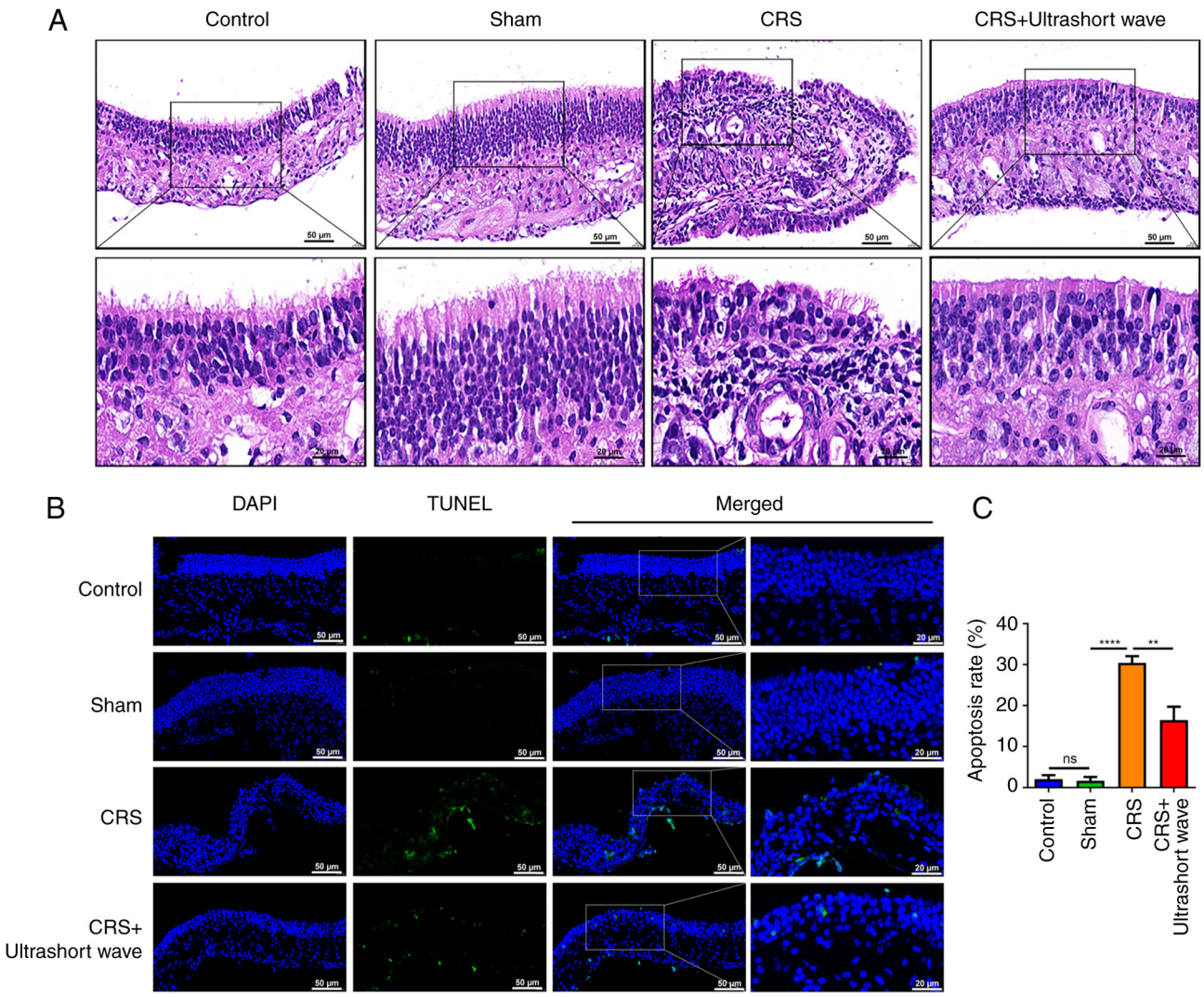

Figure 1. Ultrashort wave therapy improves histopathology and inhibits apoptosis in sinus mucosal samples. (A) Hematoxylin and eosin staining revealed the pathological changes in sinus mucosal samples. (B and C) Apoptosis in sinus mucosa across different groups was assessed using TUNEL assay. Scale bars, 50 and 20 μm. **P<0.01 and ****P<0.0001. N=6. CRS, chronic rhinosinusitis; ns, no significance.

annual healthcare visits related to CRS among children (15). Furthermore, expenditures for the treatment of CRS in children aged 12 and under soared to an astonishing $1.8 billion within a single year (16). A significant portion of these costs is associated with identifying the root cause of the disorder and determining the appropriate treatment. Considering its prevalence among the paediatric population, it is essential to formulate strategies aimed at protecting children from CRS. In the present study, the potential role and mechanisms by which ultrashort wave therapy influences the progression of CRS in a mouse model were elucidated. The findings demonstrated that ultrashort waves effectively inhibited the p38/JNK/ERK signalling pathway, leading to notable improvements in histopathological outcomes while simultaneously reducing apoptosis and inflammation within sinus mucosa.

During the progression of CRS, the sinus mucosal epithelium undergoes characteristic apoptosis and desquamation (17). This depletion of epithelial cells likely compromises the barrier function of the epithelium, rendering it more vulnerable to bacterial colonization, biofilm formation, and sustained inflammatory responses (18). Furthermore, the sinus mucosa is covered by a pseudostratified columnar ciliated epithelium. This intricate epithelial layer comprises varying proportions of goblet cells (20%), basal cells (5%), and ciliated cells (75%), all situated on an acellular basement membrane (19). The cilia play a crucial role in mucociliary clearance, a fundamental defense mechanism that ensures the proper functioning of the paranasal sinuses. Effective mucociliary clearance relies on coordinated ciliary movement and adequate glandular secretions, both indispensable for maintaining healthy sinus mucosa (20,21). In the present study, the damaged ciliary structures within the sinus mucosa of mice with CRS exhibited significant repair following ultrashort wave intervention, characterized by a well-organized arrangement. Furthermore, the apoptotic epithelial cells in the sinus mucosa of mice with CRS demonstrated a notable reversal when subjected to ultrashort wave therapy. These findings suggest that ultrashort wave intervention may effectively improve ciliary structures and reduce apoptosis in the sinus mucosa during the progression of CRS.

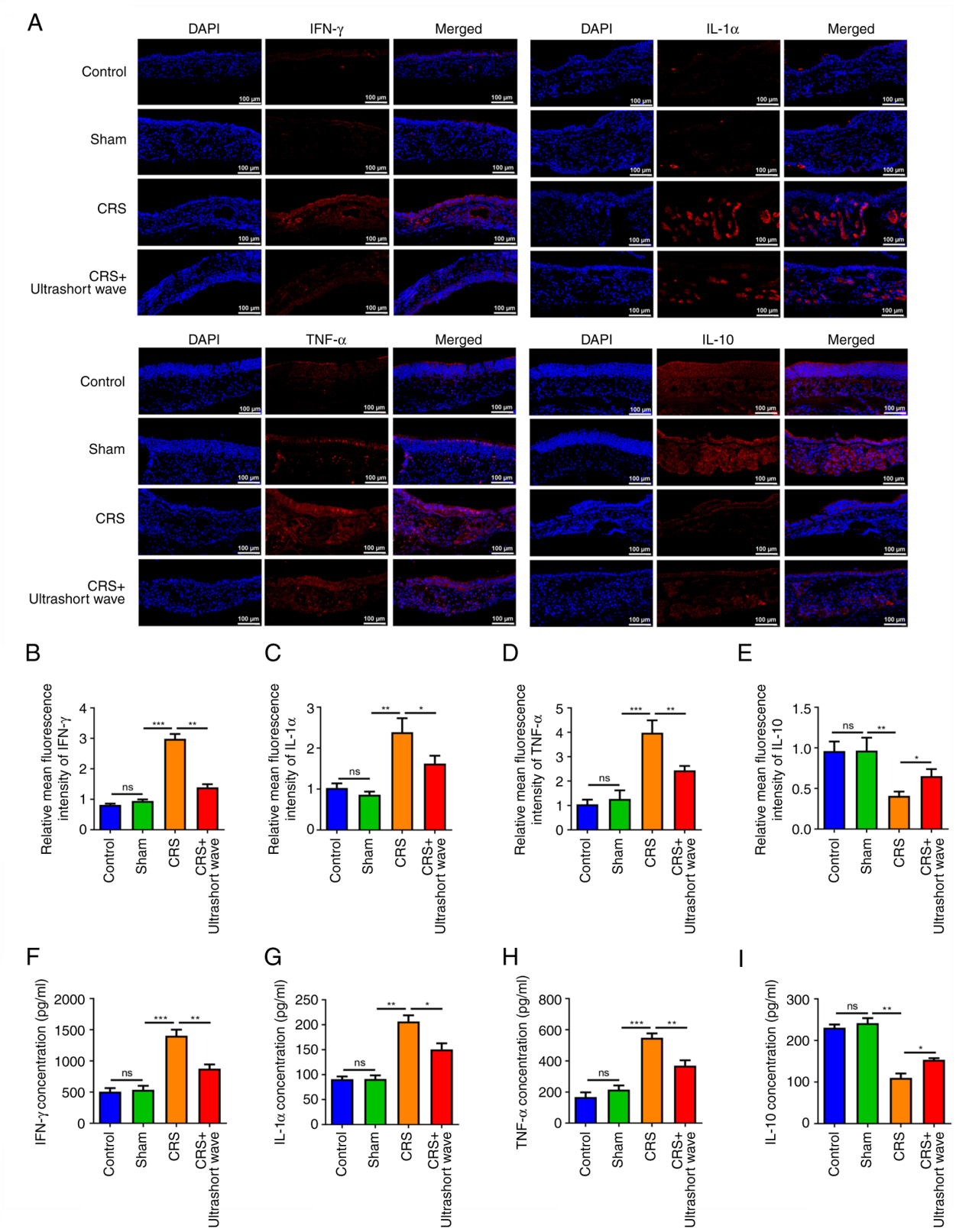

Figure 2. Ultrashort wave therapy inhibits inflammatory responses in the sinus mucosal samples of mice with CRS. (A-E) Immunofluorescence was performed to assess the expression levels of IFN-γ, IL-1α, TNF-α, and IL-10 in sinus mucosal samples of mice with CRS. (F-I) The concentrations of IFN-γ, IL-1α, TNF-α, and IL-10 in nasal lavage fluid of mice with CRS were measured using ELISA. Scale bar, 100 μm. *P<0.05, **P<0.01 and ***P<0.001. N=6. CRS, chronic rhinosinusitis; ns, no significance.

Another notable characteristic of CRS is the persistent inflammatory responses that occur within the sinuses. Studies have demonstrated that the sinus mucosal epithelium plays a pivotal role in the inflammatory cascades during CRS by secreting a wide range of pro-inflammatory cytokines, including IFN-γ, IL-1α, and TNF-α as well as

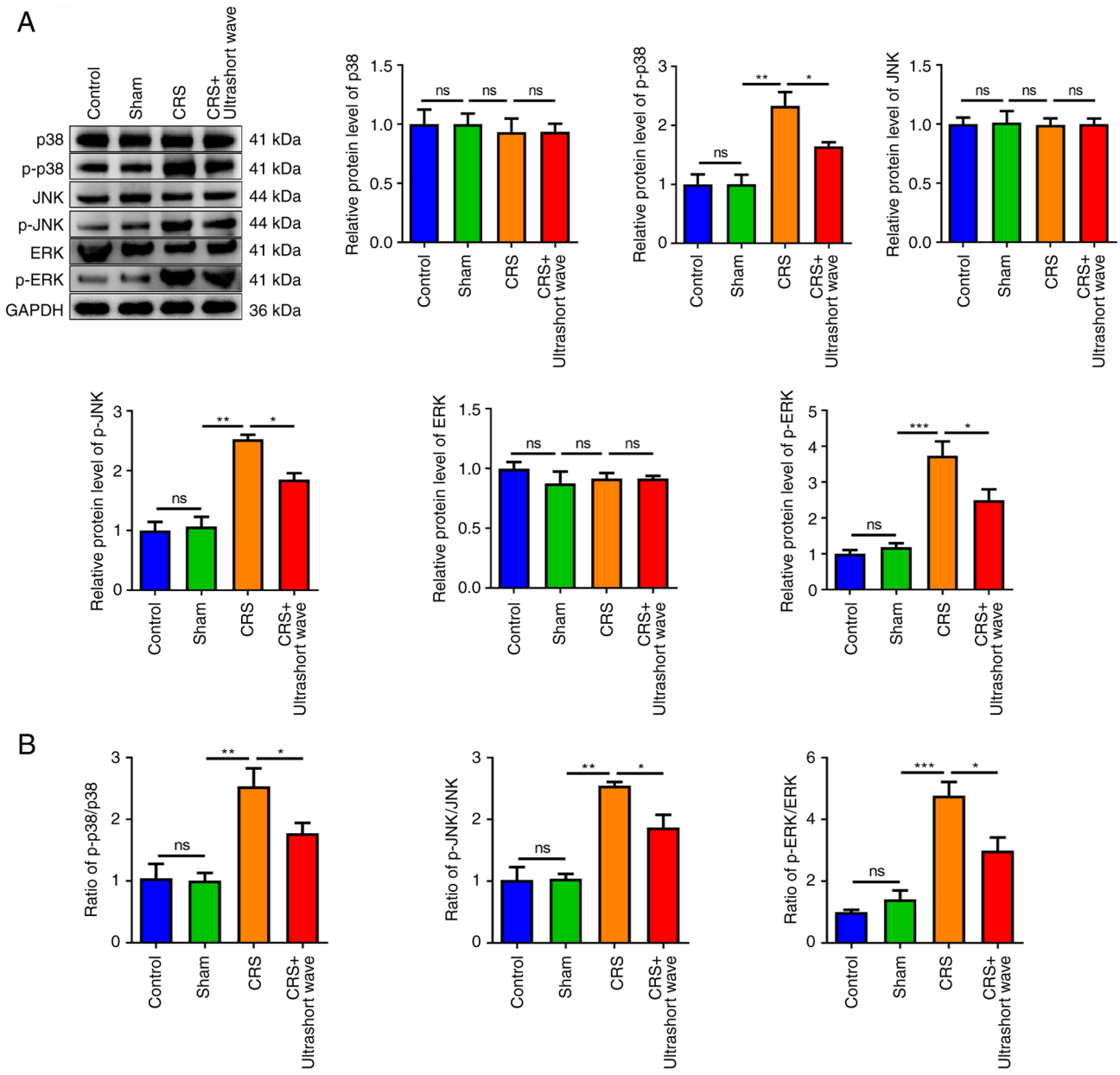

Figure 3. Ultrashort wave therapy inhibits the p-38/JNK/ERK pathway in mice with CRS. (A) The protein levels of p38, p-p38, JNK, p-JNK, ERK and p-ERK in the sinus mucosal samples of mice with CRS were determined using western blotting. (B) The ratios of p-38/p38, p-JNK/JNK and p-ERK/ERK were assessed. *P<0.05, **P<0.01 and ***P<0.001. N=6. CRS, chronic rhinosinusitis; ns, no significance.

anti-inflammatory cytokine IL-10 (22). TNF-α, a multifunctional cytokine known for its pro-inflammatory properties, can be synthesized by epithelial cells and may further stimulate the production of IL-1α and IFN-γ (23). Activated T cells promote the expression of these pro-inflammatory cytokines in epithelial cells. High levels of IFN-γ can induce apoptosis in highly activated epithelial cells (24). The primary biological function of IL-10 is to suppress antigen presentation by macrophages and dendritic cells, as well as to inhibit TNF-α production by Th1 lymphocytes (25). Furthermore, IL-10 can block the effects of IL-1α through the release of its receptor antagonists (26). These data suggest that during the development of CRS, the levels of IFN-γ, IL-1α and TNF-α are elevated, whereas IL-10 levels are reduced. This finding is consistent with our observations. Moreover, the findings in the present study further indicated that ultrashort wave intervention significantly decreased the levels of IFN-γ, IL-1α, and TNF-α, while markedly increasing the level of IL-10. These results revealed a notable anti-inflammatory effect associated with ultrashort wave therapy throughout the progression of CRS. Currently, the importance of the increased phosphorylation of p38, JNK and ERK has been demonstrated in various human inflammatory diseases (27-29). Notably, numerous studies have respectively reported the roles of the three signaling factors, p38, JNK and ERK, in CRS. For example, Lee *et al* (30) reported that increased levels of p-p38 exacerbate CRS by inducing epithelial-mesenchymal transition. Victores *et al* (31) reported that olfactory loss in CRS is associated with the activation of JNK. Wu *et al* (32) found that the occurrence of inflammatory responses is accompanied by the activation of

ERK. Considering the anti-apoptotic and anti-inflammatory roles of ultrashort wave therapy in the progression of CRS, it was therefore hypothesized that the p38/JNK/ERK signalling pathway may be an important intracellular target of ultrashort wave therapy in inhibiting the development of CRS. As anticipated, the phosphorylation levels of p38, JNK, and ERK were significantly elevated in the sinus mucosa of mice with CRS. However, these levels were markedly reduced following ultrashort wave therapy.

There are several limitations in the present study that should be addressed in future research. Numerous studies have reported the role of NF-κB and PI3K/Akt signalling in the progression of CRS (33-35). In addition, NF-κB and PI3K/Akt have been reported to be regulated by ultrashort wave therapy in some inflammation-related diseases such as spinal cord injury (36). However, the interaction between the p38/JNK/ERK signalling pathway and ultrashort wave therapy in the progression of CRS has rarely been investigated. Therefore, exploring the role of the p38/JNK/ERK signalling pathway in the present study may be considered a somewhat subjective choice. In the future, apart from the p38/JNK/ERK signalling pathway, exploring the effects of ultrashort wave therapy on other pathways involved in CRS, such as NF-κB or PI3K/Akt would strengthen the novelty of the findings. Additionally, adult C57BL/6J mice aged 8-10 weeks were used for modelling in the present study. By contrast, the immune system, nasal cavity, and sinus structure of juvenile mice (particularly those under 6-8 weeks of age) are still in the developmental stages. For instance, the sinus mucosa is not fully mature, and the functionality of immune cells has yet to be completely established. Modeling may lead to additional lesions and even mortality in juvenile mice. Furthermore, during the modeling process, these young mice may undergo rapid growth and development, which could disrupt the stability of disease progression. Therefore, translating these findings into clinical practice, particularly in paediatric patients, presents several potential challenges. First, species and developmental differences must be carefully considered, as results obtained from mouse models may not fully apply to human paediatric patients due to anatomical and immunological disparities. Thus, the specific mechanisms identified in animal studies require validation in pediatric populations. Second, compliance and sedation pose practical obstacles, since young children may struggle to remain still during treatment, necessitating sedation that carries anesthesia-related risks. Finally, long-term safety remains a critical concern, and thus extended follow-up in preclinical and clinical trials is essential.

In summary, the present study provides preliminary insights into the potential role and mechanisms of ultrashort wave therapy in the progression of CRS in mice. This therapeutic approach exhibited a notable protective effect during CRS progression. It can mitigate inflammation and apoptosis as well as protect the integrity of ciliary structures in sinus mucosa by inhibiting the activation of the p38/JNK/ERK signalling pathway. Consequently, ultrashort wave therapy may serve as a promising avenue for developing effective treatments for CRS, either as an independent intervention or in combination with other pharmacological agents.

Acknowledgements

Not available.

Funding

The present study was supported by Key Projects of Jinhua Science and Technology Bureau (grant no. 2022-3-003).

Availability of data and materials

The data generated in the present study may be requested from the corresponding author.

Authors' contributions

HX made substantial contributions to the conception and design of the study. All authors (HX, JW, QB, YJ, CX, and LC) made substantial contributions to the acquisition, analysis, and interpretation of data in the present study. HX drafted the manuscript. JW, QB, YJ, CX, and LC confirm the authenticity of all the raw data. All authors revised the manuscript critically for important intellectual content, read and approved the final version of the manuscript, and agree to be accountable for all aspects of the work in ensuring that questions related to the accuracy or integrity of any part of the work are appropriately investigated and resolved.

Ethics approval and consent to participate

Animal experiments were conducted in compliance with the guidelines outlined in the NIH Guide for the Care and Use of Laboratory Animals and approved (approval no. 20220601001) by the Ethics Committee of Lanxi People's Hospital (Lanxi, China).

Patient consent for publication

Not applicable.

Competing interests

The authors declare that they have no competing interests.

References

1. Wallace DV: Treatment options for chronic rhinosinusitis with nasal polyps. Allergy Asthma Proc 42: 450-460, 2021.
2. Snidvongs K, Sangubol M and Poachanukoon O: Pediatric versus adult chronic rhinosinusitis. Curr Allergy Asthma Rep 20: 29, 2020.
3. Ramadan HH: Pediatric chronic rhinosinusitis. Eur Arch Otorhinolaryngol 281: 1131-1137, 2024.
4. Poachanukoon O, Nanthapisal S and Chaumrattanakul U: Pediatric acute and chronic rhinosinusitis: Comparison of clinical characteristics and outcome of treatment. Asian Pac J Allergy Immunol 30: 146-151, 2012.
5. Siddiqui Z, Tahiri M, Gupta A, Kin Nam RH and Rachmanidou A: The management of paediatric rhinosinusitis. Int J Pediatr Otorhinolaryngol 147: 110786, 2021.
6. Ventriglia G, Gervasoni F, Franco M, Magni A, Panico G and Iolascon G: Musculoskeletal pain management and thermotherapy: An exploratory analysis of italian physicians' attitude, beliefs, and prescribing habits. J Pain Res 16: 1547-1557, 2023.

7. Yang X, Li K, Li M, Chen C, Yang X, Li J and Zhang H: Ultrashort wave diathermy inhibits pulmonary inflammation in mice with acute lung injury in a HSP70 independent way: A pilot study. Mol Biol Rep 51: 750, 2024.
8. Yu HPM, Jones AY, Dean E and Liisa Laakso E: Ultra-shortwave diathermy-a new purported treatment for management of patients with COVID-19. Physiother Theory Pract 36: 559-563, 2020.
9. Kong L, Zhang JL and Zhu CM: Ultrashort wave therapy for chronic rhinosinusitis with nasal polyps: protocol for a randomized, double-blind, sham-controlled trial. Trials 26: 391, 2025.
10. Fouda KZ, Eladl HM, Ameer MA and Allam NM: Effect of adding physiotherapy program to the conservative medical therapy on quality of life and pain in chronic rhinosinusitis patients. Ann Rehabil Med 47: 393-402, 2023.
11. National Research Council (US) Committee for the Update of the Guide for the Care and Use of Laboratory Animals: Guide for the Care and Use of Laboratory Animals, 8th edition. National Academies Press (US), Washington, DC, 2011.
12. Geng L, Wang S, Zhao Y and Hu H: Gene expression profile in mouse bacterial chronic rhinosinusitis. Exp Ther Med 17: 3451-3458, 2019.
13. Yu H, Huang X, Xie C, Song J, Zhou Y, Shi H, Chen M, Wu Y, Ruan Z, Deng L, *et al*: Transcriptomics reveals apigenin alleviates airway inflammation and epithelial cell apoptosis in allergic asthma via MAPK pathway. Phytother Res 37: 4002-4017, 2023.
14. Makary CA, Tumlin P, Asad F, Wasef K and Ramadan HH: Quality of life measurement for adolescent patients with sinonasal symptoms. Laryngoscope 133: 1052-1058, 2023.
15. Levy DA, Pecha PP, Nguyen SA and Schlosser RJ: Trends in complications of pediatric rhinosinusitis in the United States from 2006 to 2016. Int J Pediatr Otorhinolaryngol 128: 109695, 2020.
16. Mirza AA, Shawli HY, Alandejani TA, Aljuaid SM, Alreefi M, Basonbul RA, Alhomaiani SK, Althobaity BA, Alhumaidi DA and Zawawi F: Efficacy and safety of paranasal sinus balloon catheter dilation in pediatric chronic rhinosinusitis: A systematic review. J Otolaryngol Head Neck Surg 49: 69, 2020.
17. Ma X, Guo S, Liu F, Li C, Shi X, Liu W, Qi L, Yuan Y, Xie X, Wang P, *et al*: Unveiling the prevalence and impact of silent rhinovirus infection in chronic rhinosinusitis with nasal polyps. Ann Allergy Asthma Immunol 134: 420-430.e1, 2025.
18. Song J, Wang M, Wang C and Zhang L: Olfactory dysfunction in chronic rhinosinusitis: Insights into the underlying mechanisms and treatments. Expert Rev Clin Immunol 19: 993-1004, 2023.
19. Ruysseveldt E, Martens K and Steelant B: Airway basal cells, protectors of epithelial walls in health and respiratory diseases. Front Allergy 2: 787128, 2021.
20. Alekseenko S, Karpischenko S and Barashkova S: Comparative analysis of mucociliary clearance and mucosal morphology using high-speed videomicroscopy in children with acute and chronic rhinosinusitis. Am J Rhinol Allergy 35: 656-663, 2021.
21. Chegini Z, Noei M, Hemmati J, Arabestani MR and Shariati A: The destruction of mucosal barriers, epithelial remodeling, and impaired mucociliary clearance: Possible pathogenic mechanisms of Pseudomonas aeruginosa and Staphylococcus aureus in chronic rhinosinusitis. Cell Commun Signal 21: 306, 2023.
22. Wang C, Yan B and Zhang L: The epithelium-derived inflammatory mediators of chronic rhinosinusitis with nasal polyps. Expert Rev Clin Immunol 16: 293-310, 2020.
23. Mitoma H, Horiuchi T, Tsukamoto H and Ueda N: Molecular mechanisms of action of anti-TNF-α agents-comparison among therapeutic TNF-α antagonists. Cytokine 101: 56-63, 2018.
24. Chufistova AV, Shabaldina EV, Bedareva AV, Vakhrameev IN, Abramova NA and Shabaldin AV: Features of inflammatory endotypes and phenotypes in chronic rhinosinusitis. Vestn Otorinolaringol 89: 60-67, 2024 (In Russian).
25. Xuan L, Zhang N, Wang X, Zhang L and Bachert C: IL-10 family cytokines in chronic rhinosinusitis with nasal polyps: From experiments to the clinic. Front Immunol 13: 947983, 2022.
26. Liang Y, Yin S, Chen X, Li C and Chen Q: The causal relationship between autoimmune diseases and rhinosinusitis, and the mediating role of inflammatory proteins: A Mendelian randomization study. Exp Biol Med (Maywood) 249: 10196, 2024.
27. Yue Q, Liu T and Cheng Z: Protective effect of colchicine on LPS-induced lung injury in rats via inhibition of P-38, ERK1/2, and JNK activation. Pharmacology 105: 639-644, 2020.
28. Jang EJ, Kim H, Baek SE, Jeon EY, Kim JW, Kim JY and Kim CD: HMGB1 increases RAGE expression in vascular smooth muscle cells via ERK and p-38 MAPK-dependent pathways. Korean J Physiol Pharmacol 26: 389-396, 2022.
29. Fawzy MA, Maher SA, Bakkar SM, El-Rehany MA and Fathy M: Pantoprazole attenuates MAPK (ERK1/2, JNK, p38)-NF-κB and apoptosis signaling pathways after renal ischemia/reperfusion injury in rats. Int J Mol Sci 22: 10669, 2021.
30. Lee M, Kim DW, Khalmuratova R, Shin SH, Kim YM, Han DH, Kim HJ, Kim DY, Rhee CS, Park JW and Shin HW: The IFN-γ-p38, ERK kinase axis exacerbates neutrophilic chronic rhinosinusitis by inducing the epithelial-to-mesenchymal transition. Mucosal Immunol 12: 601-611, 2019.
31. Victores AJ, Chen MF, Smith A and Lane AP: Olfactory loss in chronic rhinosinusitis is associated with neuronal activation of c-Jun N-terminal kinase. Int Forum Allergy Rhinol 8: 415-420, 2018.
32. Wu YS, Sun KY, Tu YY, Li P, Hao D, Yu P, Chen A, Wan Y and Shi L: miR-200a-3p regulates epithelial-mesenchymal transition and inflammation in chronic rhinosinusitis with nasal polyps by targeting ZEB1 via ERK/p38 pathway. Int Forum Allergy Rhinol 14: 41-56, 2024.
33. Chen W, Liu ZJ and Ye J: Relationship among the expression of GSK3β, PI3K/Akt, and IL-6 in chronic rhinosinusitis. Zhonghua Er Bi Yan Hou Tou Jing Wai Ke Za Zhi 48: 128-134, 2013 (In Chinese).
34. Yang HW, Kim HJ, Park JH, Shin JM and Lee HM: Apigenin alleviates TGF-β1-induced nasal mucosa remodeling by inhibiting MAPK/NF-kB signaling pathways in chronic rhinosinusitis. PLoS One 13: e0201595, 2018.
35. Chen XH, Chang LH, Li X, Huang J, Yang L, Lai X, Huang Z, Wang Z, Wu X, Zhao J, *et al*: Tc17/IL-17A Up-regulated the expression of MMP-9 via NF-κB pathway in nasal epithelial cells of patients with chronic rhinosinusitis. Front Immunol 19: 2121, 2018.
36. Wang S, Jia Y, Cao X, Feng S, Na L, Dong H, Gao J and Zhang L: HUCMSCs transplantation combined with ultrashort wave therapy attenuates neuroinflammation in spinal cord injury through NUR77/NF-κB pathway. Life Sci 267: 118958, 2021.